Carbonyl Posttranslational Modification Associated With Early-Onset Type 1 Diabetes Autoimmunity

Mei-Ling Yang,[1] Sean E. Connolly,[1] Renelle J. Gee,[1] TuKiet T. Lam,[2,3] Jean Kanyo,[2] Jian Peng,[4] Perrin Guyer,[5] Farooq Syed,[6] Hubert M. Tse,[7] Steven G. Clarke,[8] Catherine F. Clarke,[8] Eddie A. James,[5] Cate Speake,[9] Carmella Evans-Molina,[6] Peter Arvan,[10] Kevan C. Herold,[4,11] Li Wen,[4] and Mark J. Mamula[1]

Diabetes 2022;71:1979–1993 | https://doi.org/10.2337/db21-0989

Inflammation and oxidative stress in pancreatic islets amplify the appearance of various posttranslational modifications to self-proteins. In this study, we identified a select group of carbonylated islet proteins arising before the onset of hyperglycemia in NOD mice. Of interest, we identified carbonyl modification of the prolyl-4-hydroxylase β subunit (P4Hb) that is responsible for proinsulin folding and trafficking as an autoantigen in both human and murine type 1 diabetes. We found that carbonylated P4Hb is amplified in stressed islets coincident with decreased glucose-stimulated insulin secretion and altered proinsulin-to-insulin ratios. Autoantibodies against P4Hb were detected in prediabetic NOD mice and in early human type 1 diabetes prior to the onset of anti-insulin autoimmunity. Moreover, we identify autoreactive CD4$^+$ T-cell responses toward carbonyl-P4Hb epitopes in the circulation of patients with type 1 diabetes. Our studies provide mechanistic insight into the pathways of proinsulin metabolism and in creating autoantigenic forms of insulin in type 1 diabetes.

Type 1 diabetes (T1D) is an organ-specific autoimmune disease marked by lymphocyte infiltration of pancreatic islets. Insulitis results in the liberation of reactive oxygen species (ROS) and induces the production of proinflammatory cytokines. Accumulating evidence in both experimental and clinical studies demonstrates that oxidative stress induced by hyperglycemia and insulitis plays a key role in the onset of T1D and diabetes-related complications of disease (1,2). For example, islet proteins exposed to metal-catalyzed oxidation generate GAD65 aggregates that react with serum autoantibodies from patients with T1D (3). Moreover, antioxidants delay and/or prevent the onset of T1D spontaneously in NOD and streptozotocin-induced T1D murine models (4,5). Of interest, oxidative stress usually accompanies a wide spectrum of protein posttranslational modifications (PTMs), such as carbonylation, hydroxylation, nitrosylation, and glutathionylation (6). PTMs are known as one mechanism by which autoreactive T and B cells escape selection and break tolerance to neo self-proteins (1). In the current study, we examine protein modifications induced by inflammation and oxidative stress leading to neoautoantigens in T1D.

Protein carbonylation is a major product of tissue proteins in response to oxidative stress. Both oxidative stress and protein carbonylation contribute to insulin resistance and metabolic dysfunctions in adipose tissue of both animal

[1]Section of Rheumatology, Allergy and Immunology, Department of Internal Medicine, Yale University, New Haven, CT
[2]Mass Spectrometry & Proteomics Resource, W.M. Keck Foundation Biotechnology Resource Laboratory, New Haven, CT
[3]Department of Molecular Biophysics and Biochemistry, Yale University, New Haven, CT
[4]Section of Endocrinology, Department of Internal Medicine, Yale University, New Haven, CT
[5]Center for Translational Immunology, Benaroya Research Institute at Virginia Mason, Seattle, WA
[6]Center for Diabetes and Metabolic Diseases, Indiana University School of Medicine, Indianapolis, IN
[7]Department of Microbiology, Comprehensive Diabetes Center, University of Alabama at Birmingham, Birmingham, AL
[8]Department of Chemistry and Biochemistry, University of California, Los Angeles, Los Angeles, CA
[9]Center for Interventional Immunology, Benaroya Research Institute at Virginia Mason, Seattle, WA
[10]Department of Internal Medicine, University of Michigan, Ann Arbor, MI
[11]Department of Immunobiology, Yale University, New Haven, CT

Corresponding author: Mark J. Mamula, mark.mamula@yale.edu

Received 3 November 2021 and accepted 15 June 2022

This article contains supplementary material online at https://doi.org/10.2337/figshare.20103134.

models and human T1D (7). Carbonylation leads to sarco(endo)plasmic reticulum Ca^{2+}-ATPase 2a activity loss and diastolic dysfunction in the streptozotocin-induced T1D murine model (8). Recent studies profiled carbonylated plasma proteins as potential biomarkers in type 2 diabetes (6,9). Little is known about the role of carbonylated neoantigens in the progression of T1D.

In this study, proteomic analysis identified 23 carbonylated islet polypeptides unique to prediabetic NOD mice. Seven of these polypeptides were recognized by serum antibodies from prediabetic NOD mice, including protein disulfide isomerase (PDI) isoforms, 14–3-3 protein isoforms, glucose-regulated protein 78 (GRP78), and chymotrypsinogen B. Of interest, prolyl-4-hydroxylase β subunit (P4Hb; also known as PDIA1) was found to be an early autoantigen in both human and murine models of T1D. P4Hb is required for proinsulin maturation and pancreatic β-cell health (10). Our data suggest a novel role of P4Hb as an early target of autoimmunity. As discussed in this study, modified P4Hb biological functions provide one explanation for recent observations of increased proinsulin to insulin ratios in the progression of T1D (11).

RESEARCH DESIGN AND METHODS

Samples From Animals and Humans With T1D

NOD/ShiLt, BALB/c, and C57BL/6 female mice were purchased at 3 weeks of age from The Jackson Laboratory (Bar Harbor, ME). Blood glucose values >250 mg/dL were considered diabetic. Murine pancreatic islets were handpicked from 5-week-old NOD mice.

Three sets of human samples were used in this study.

1. For anti-P4Hb antibody and anti-insulin (auto)antibody by ELISA, human serum samples were collected from early-onset disease (n = 21; under 1 year of disease duration; all are children/toddlers <14 years of age) and healthy control subjects (n = 10; 6 women; median age 43 years, range 29–58 years). Eight out of 21 patients with early-onset T1D were collected for serum at different time point before and/or after insulin treatment (1, 3, 6, 9, and 12 months), with written informed consent.
2. For anti-P4Hb and anticarbonyl-P4Hb antibodies by ELISA, human serum samples were collected from subjects diagnosed with established T1D (n = 18; 7 women; median age 15 years, range 6–70 years; 2.7–55 years of disease duration) and healthy control subjects (n = 14; 6 women; median age 32 years, range 23–59 years). Samples were assayed in a blinded fashion for ELISA as described below. The presence or absence of antibodies against GAD65, IA2, ZnT8, and insulin was determined by the Barbara Davis Center Autoantibody/HLA Service Center using standardized radioimmunoassay.
3. For HLA tetramer-based T-cell assays, peripheral blood was collected from 11 individuals with T1D with DRB1*04:01 haplotypes after obtaining written consent under a study approved by the Institutional Review Board at the Benaroya Research Institute or Universitair Ziekenhuis Leuven. Subject attributes are summarized in Supplementary Table 1.

Human Islet Culture and Glucose Stimulation Insulin/Proinsulin Assay

Human islets were obtained from cGMP Human Cell Processing Facility (Diabetes Research Institute, University of Miami) in accordance with ethical regulations. Six donors were 25–53 years old with no history of diabetes or other pancreatic disease. To model pancreas inflammation, islets (2,000 islet equivalents/well on a 12-well plate) were cultured in CMRL 1066–supplemented medium (Gibco; contains 5.5 mmol/L glucose, 10% FBS, 10 mmol/L HEPES, 2 mmol/L L-glutamine, and 1% penicillin/streptomycin) in the presence of 500 μmol/L H_2O_2 for 1 h or recombinant human interferon-γ (rhIFN-γ; 1,000 U/mL), interleukin-1β (rhIL-1β; 50 U/mL), and tumor necrosis factor-α (rhTNF-α; 1,000 U/mL) for 68–72 h. Then, islets were washed with PBS and cultured with CMRL 1066–supplemented medium with low (5.5 mmol/L) or high (16.7 mmol/L) glucose for 1 h (12). Supernatants were then assayed for insulin and proinsulin concentration by commercial ELISA (ALPCO, Inc., Salem, NH).

Differential Two-Dimensional Gel Electrophoresis

NOD islet protein extracts were separated by standard two-dimensional (2D) gel electrophoresis by using ZOOM IPGRunner first-dimension isoelectric focusing (IEF) unit (Invitrogen, Waltham, MA) and followed by second-dimension 12.5% SDS-PAGE. Prior to IEF, proteins were precipitated away from detergents, salts, lipids, and nucleic acids using the 2-D Clean-Up Kit (GE Healthcare, Pittsburgh, PA). After IEF, strips were alkylated with 125 mmol/L iodoacetamide for 15 min on a rotary shaker at room temperature (Sigma-Aldrich, St. Louis, MO). Second-dimension resolution was carried out by standard SDS-PAGE, followed by protein staining and transfer to nitrocellulose for immunoblotting. We performed silver staining of 2D gels prior to spot excision and mass spectroscopy (SilverQuest; Invitrogen).

Detection of Carbonyl Modification by OxyBlot

Protein carbonylation from islet lysates was detected with the OxyBlot Protein Oxidation Detection Kit (Millipore). Briefly, carbonyl groups were derivatized by 2,4-dinitrophenylhydrazine (DNPH) to form a stable dinitrophenyl (DNP) hydrazone product by the manufacturer's protocol and were then detected by anti-DNP antibodies.

Identification of the Carbonyl Modification of P4Hb by DNPH-Assisted Mass Spectrometry

rhP4Hb was incubated in PBS or PBS containing 100 μmol/L $FeSO_4$, 25 mmol/L H_2O_2, and 25 mmol/L ascorbate (oxidative condition) as described (13). The native and oxidative rhP4Hb samples were derivatized with DNPH (14). In brief, rhP4Hb was incubated with 5 mmol/L DNPH/PBS and neutralized with 0.5 mmol/L Tris base. DNPH-derivatized

rhP4Hb was digested with trypsin, rederivatized with DNPH, and incubated in the presence or absence of 15 mmol/L sodium cyanoborohydride prior to liquid chromatography–tandem mass spectrometry (LC-MS/MS) analysis. Without stabilizer, mass shifts of 136.97, 194.11, 179.02, and 178.01 identified DNPH-derivatized carbonyl groups of arginine, proline, lysine, and threonine, respectively (15). With stabilizer, 2 Da was added to the mass shifts for each residue (16). LC-MS/MS analysis was performed on a Q Exactive Plus spectrometer as described (17). MS/MS spectra were searched using Proteome Discoverer software (Thermo Fisher Scientific, Waltham, MA) linked to the automated MASCOT (Matrix Science Inc, Boston, MA) algorithm against the National Center for Biotechnology Information nr database and manually validated using Scaffold PTM.

Detection of Carbonylated P4Hb and Oxidative Status by Flow Cytometry and Confocal Microscopy

Islet cells or INS-1 cells were first stained with rabbit monoclonal anti-P4Hb (ab137110; Abcam) and anti-rabbit Alexa Fluor 647 (A21244; Life Technologies). Cells were then treated with 1 mmol/L DNPH (Fluka) or 2N HCl derivatization buffer, followed by staining with goat anti-DNP (D9781; Sigma-Aldrich) and anti-goat Alexa Fluor 488 (ab150129; Abcam). Intracellular ROS level was measured by CellROX Deep Red probe (Molecular Probes). Both carbonylation and ROS level were analyzed by FACSCalibur (BD Biosciences) with FlowJo software (Tree Star).

Human islet suspension was applied to Alcian blue–coated slides, fixed with 2% paraformaldehyde, washed twice with PBS, and permeabilized with 0.3% Triton X-100. Islets were treated with DNPH or HCl in staining buffer (PBS/BSA/Tween-20/SDS). After derivatization, the islets were stained with anti-insulin (A21434; R&D Systems), anti-P4Hb, and anti-DNP as described above and analyzed on a Leica SP5 II confocal microscope.

ELISA and Immunoblot Assay

Human and mouse anti-P4Hb was performed by ELISA. Briefly, 1 μg of recombinant human P4Hb protein or insulin (GeminiBio) in carbonate buffer was coated onto microtiter plates and blocked with 1% BSA in 1% Tween PBS for mouse anti-P4Hb and commercial Blocker Casein (Pierce Biotechnology, Rockford, IL) for human anti-P4Hb. Anti-insulin antibodies were assessed by the Barbara Davis Center for Childhood Diabetes (University of Colorado, Anschutz Medical Campus) or as previously published (see figure/table legends) (18). Serum dilutions were incubated 2 h at room temperature followed by goat anti-IgG or anti-IgM alkaline phosphatase (SouthernBiotech), developed with para-nitrophenyl phosphate substrate (Sigma-Aldrich), and read at 405 nm (BioTek Instruments). Individual signals were normalized to no-antigen control wells. All readings were normalized to nonspecific serum binding to no-antigen control wells. Positive signals were >2 SD above BALB/c serum or human healthy serum.

For immunoblotting, protein samples (pancreatic islet extract isolated from NOD mice) were separated via 2D SDS-PAGE, blotted onto a nitrocellulose membrane, and probed with serum (1:100) from NOD mice or patients with T1D, incubated with the alkaline phosphatase–conjugated anti-mouse or anti-human IgG, and then visualized by nitro blue tetrazolium/5-bromo-4-chloro-3-indolyl phosphate substrate (Thermo Fisher Scientific).

HLA Binding Measurements and HLA Class II Tetramer Preparation

DRB1*04:01 protein was purified from insect cell cultures in either nonbiotinylated (for competition assays) or biotinylated (for tetramer preparation) form as previously described (19). A previously published competition assay was used to measure the binding of wild-type (P4Hb 96–114 VRGYPTIKFFKNGDTASPKE) or carbonylated p4Hb peptide (P4Hb 96–114 VRGYP[T]IKFFKNGDTASPKE, carbonylated at position 101; Mimotopes, Clayton, VIC, Australia) (20). Briefly, increasing concentrations of each peptide were incubated in competition with a biotinylated reference influenza hemagglutinin peptide (HA306-318) at 0.02 μmol/L in wells coated with DRB1*04:01 protein. After washing, residual biotin-HA was detected using Europium-conjugated streptavidin (PerkinElmer, Waltham, MA) and quantified using a Victor Nivo time-resolved fluorometer (PerkinElmer). Curves were simulated using Prism software (version 9.3; GraphPad Software Inc., San Diego, CA) and IC_{50} values calculated as the concentration needed to displace 50% of the reference peptide. To prepare tetramers, biotinylated DRB1*04:01 protein was loaded with 0.2 mg/mL peptide at 37°C for 72 h in the presence of 0.2 mg/mL *N*-dodecyl-β-maltoside and 1 mmol/L Pefabloc (Sigma-Aldrich). Peptide-loaded monomers were conjugated into tetramers using R-phycoerythrin streptavidin (Invitrogen) at a molar ratio of 8:1 and used to stain in vitro–expanded T cells.

Analysis of Human Primary T-Cell Responses and T-Cell Clones

Peripheral blood mononuclear cells (PBMCs) were isolated by Ficoll underlay, counted, and frozen in 7% DMSO until used. Samples were thawed and suspended in T-cell medium (RPMI, 10% pooled human serum, 1% penicillin-streptomycin, and 1% L-glutamine) at 4×10^6 cells/mL and stimulated with 20 μg/mL peptide in 48-well plates for 14 days, adding medium and IL-2 starting on day 7. Separate aliquots of cells were stained with phycoerythrin-labeled P4Hb T101 or irrelevant peptide-loaded tetramers for 75 min at 37°C, followed by CD4-APC (BioLegend), CD14-PerCP-Cy5.5 (Invitrogen), CD19-PerCP-Cy5.5 (BioLegend), and CD25-FITC (BioLegend) for 20 min at 4°C. Cells were run on an LSR II flow cytometer (BD Biosciences) and analyzed using FlowJo. Clones were isolated from the same expanded cultures by reactivating the cells overnight with peptide and sorting single CD154/CD69-positive $CD4^+$ T cells using an FACSAria (BD Biosciences) and then expanding in the presence of 10^5

irradiated PBMCs and phytohemagglutinin (2 μg/mL; Remel Inc.) in 96-well plates. To assess T-cell clone specificity, 10^4 T cells were plated in duplicate in the presence of 10^5 irradiated HLA-DRB1*04:01$^+$ PBMCs as antigen-presenting cells and stimulated with 10 μg/mL native or carbonylated peptide for 48 h. Then, proliferation was measured by [^{3}H]thymidine incorporation.

Statistical Analysis

All statistics were performed using a Student unpaired two-tailed *t* test unless indicated. A value of $P < 0.05$ was regarded as significant.

Data and Resource Availability

Data generated and/or analyzed in the current study are available from the corresponding author upon reasonable request. No resources were generated.

RESULTS

NOD Islet Proteomic Analyses for Carbonyl-Modified Proteins

To identify carbonyl modification in pancreatic islets prior to disease onset, pancreatic islet proteins from 5-week-old prediabetic NOD mice were investigated by 2D gel electrophoresis and probed with anti-DNP antibody. Proteins from a total of seven identified spots (Fig. 1*A*) were analyzed by LC-MS/MS and MASCOT database search. Both novel and established disease-derived autoantigens were identified with carbonyl modifications (Table 1). The list includes PDIA1 (P4Hb), PDIA2, and Hspa5 78-kDa glucose-related HSP (also known as GRP78 or BiP), all abundantly carbonylated from prediabetic NOD islets (Table 1). Of interest, pancreatic PDIA2 is an autoantigen in CTLA-4–deficient mice characterized by a fatal lymphoproliferative disorder (21). Moreover, citrullinated GRP78 has been identified as an autoantigen in T1D (22,23). Two carbonyl-modified proteins identified from prediabetic NOD islet preparations, pancreatic amylase and chymotrypsinogen, were previously identified as biomarkers for autoimmune pancreatitis and fulminant T1D (24,25), respectively.

Identification of P4Hb as an Antigenic Islet Protein

Lysates of islet cells from prediabetic NOD mice were subjected to 2D electrophoresis and immunoblotted with diabetic NOD serum (Fig. 1*B*). Protein spots bound by NOD serum were identified via LC-MS/MS following by MASCOT database analysis. By this approach, P4Hb (also known as PDIA1) was identified as one major target of autoantibodies as indicated in Fig. 1*B*. Other major carbonyl-modified target proteins identified in immunoscreen by using OxyBlot analysis and diabetic NOD serum from prediabetic NOD islet proteins were PDIA2, GRP78, 14–3-3 isoforms, and chymotrypsinogen B (highlighted with an asterisk in Table 1).

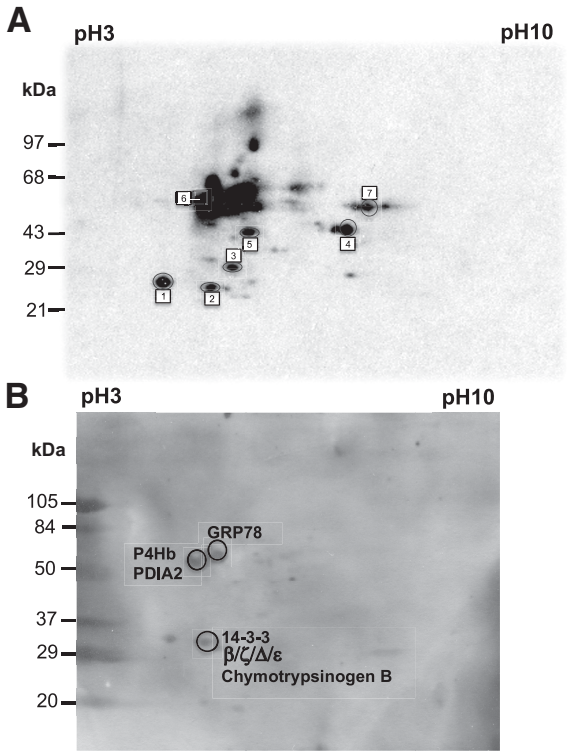

Figure 1—P4Hb is a major antigenic islet protein recognized by diabetic NOD serum. *A*: NOD islet proteomic analysis for carbonyl-modified proteins. Representative 2D blot of carbonyl-modified proteins from prediabetic NOD mice. Islet proteins from 5-week-old NOD mice were separated by IEF and derivatized with DNPH. Second-dimension separation was performed in 12.5% SDS-PAGE gels. Squares/circles and numbers indicate spots identified by LC-MS/MS. *B*: 2D immunoblot of 5-week-old NOD islet extracts was probed with serum IgG from a 20-week-old diabetic NOD mouse. The reactive islet proteins were identified by LC-MS/MS as indicated respectively. Polypeptide molecular sizes of standard proteins in kilodaltons are indicated on the left (*A* and *B*).

Oxidative and Cytokine Stress of Human Islets Induces Carbonyl Modification of P4Hb Coincident With Increased Proinsulin-to-Insulin Ratio

In modeling tissue inflammation, we incubated islets from human organ donors without diabetes with either H_2O_2 or a cocktail of proinflammatory cytokines (IFN-γ, IL-1β, and TNF-α) and assessed the induction of carbonylated P4Hb. Our results illustrate that carbonylation level was significantly elevated in human islets treated with either H_2O_2 or a cytokine cocktail compared with untreated human islets (Fig. 2*A* and *B*).

P4Hb is responsible for the retention and accurate folding of proinsulin within the endoplasmic reticulum (ER) in pancreatic β-cells (26). Thus, we next determined if carbonylated P4Hb affects metabolic functions of human β-cells, including glucose-stimulated insulin secretion. The collection and transport of human islets does impart some cellular stress, leading to carbonyl modification around the periphery of islets (green rim in Fig. 2*C*, left panel). In oxidation-

Table 1—Identification of carbonylated islet proteins in prediabetic NOD mice

Protein	pI	Spot number	Sequence coverage (%)	General biological function
Protein disulfide isomerase A1* (prolyl 4-hydroxylase subunit b)	5; 5.5; 7	2; 5; 7	8.6; 12.4; 22.2	Protein folding
Protein disulfide isomerase A2*	5.5; 4.5	5; 6	10.8; 20.7	Cellular protein modification process
Protein disulfide isomerase A6	5	3	10.3	
Hspa5 78-kDa glucose-related HSP*	5; 5.5	2; 5	5.2; 17.9	Protein folding, Hsp70 family chaperone, response to stress
14-3-3 protein β*	5	2	17.5	
14-3-3 protein γ	5	2	25.9	
14-3-3 protein η	5	2	26	Cell communication
14-3-3 protein θ	5	2	18	Chaperone
14-3-3 protein ζ/δ*	5	2	33.9	Cell cycle
14-3-3 protein ε*	5	2	18.8	
Chymotrypsinogen B*	5	2	49.8	Proteolysis/serine protease
Ubiquitin carboxyl-terminal hydrolase isozyme L3	5	2	14.3	Proteolysis/cysteine protease
Carboxypeptidase A1	5.5	5	25.1	Proteolysis/metalloprotease
Carboxypeptidase B1	5.5	5	24.8	Proteolysis/metalloprotease
Pancreatic amylase 2	7	7	38.8	Glycogen metabolism/amylase
Isocitrate dehydrogenase (NADP-dependent)	6.5	4	25.8	Carbohydrate metabolism/dehydrogenase
Methylmalonate-semialdehyde dehydrogenase (mitochondria)	7	7	9.5	Amino acid and pyrimidine
Glutamate dehydrogenase 1	7	7	14.7	Nucleobase metabolism
Carbamoyl-phosphate synthase (mitochondria)	5.5; 4.5	5; 6	1.8; 1.7	Nitrogen compound metabolism/transferase/ligase
Dihydrolipoyl dehydrogenase	7	7	9.6	Nitrogen compound metabolism, respiratory electron transport chain
Staphylococcal nuclease domain-containing protein 1	5	2	4.2	Transcription factor, nucleic acid binding
Cytosol aminopeptidase, Lap3 isoform 1	7	7	8.7	Miscellaneous
Glycine aminotransferase (mitochondria)	6.5	4	18.4	Miscellaneous

*Protein identified from immunoblot by diabetic NOD serum. pI, isoelectric point.

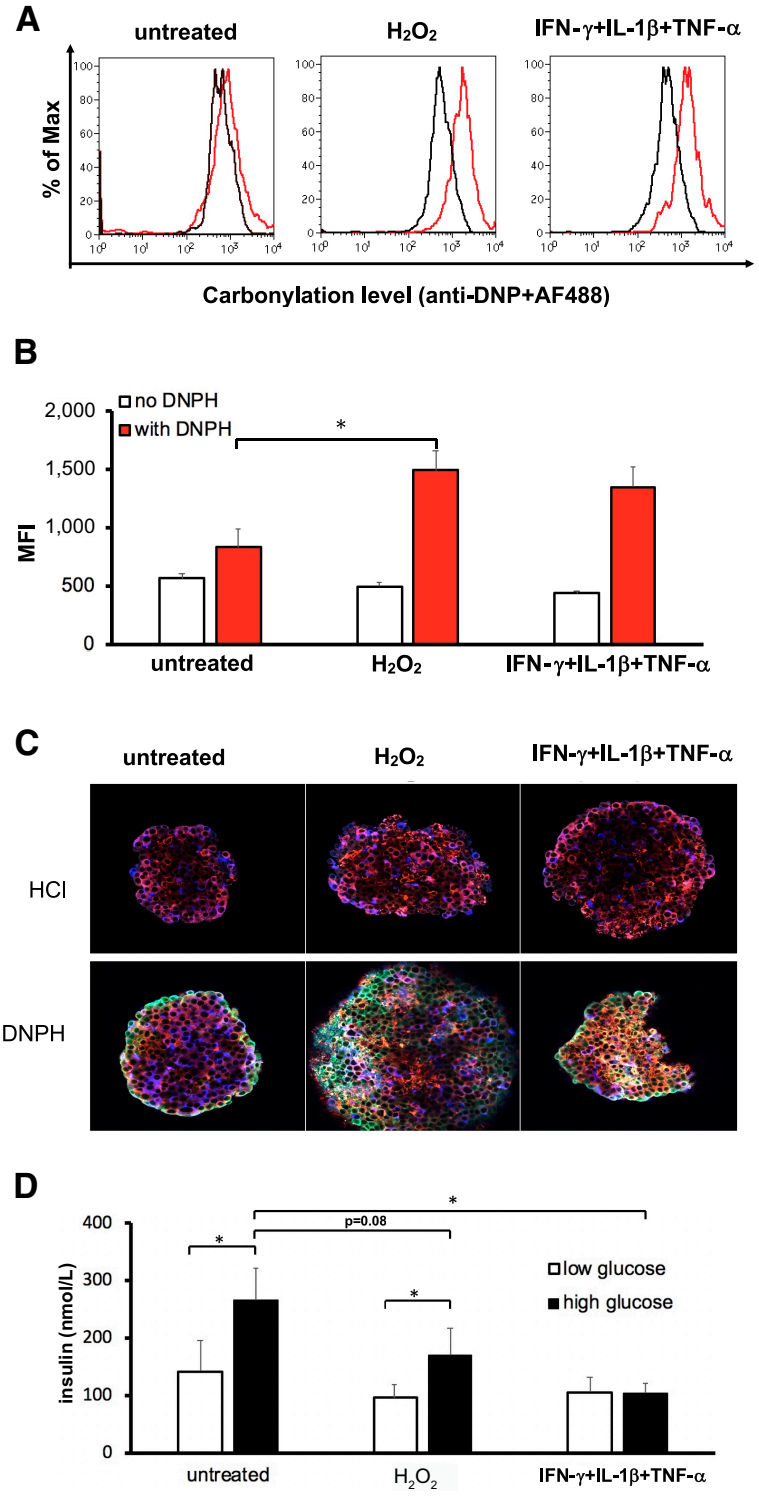

Figure 2—Continued on p. 1985.

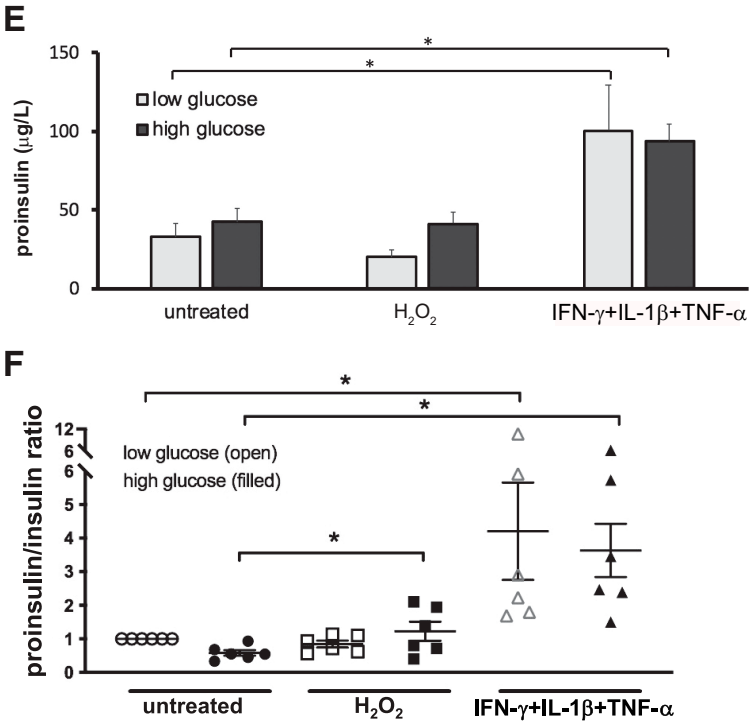

Figure 2—Increased carbonylation of P4Hb is coincident with impaired glucose-stimulated insulin secretion in stressed human islets. Human islet preparations were incubated in the presence or absence of oxidative stress (H_2O_2) or cytokine cocktail (IFN-γ+IL-1β+TNF-α) and followed by incubation of 5.5 mmol/L (low) or 16.7 mmol/L (high) glucose for 1 h. *A*: Flow cytometry analyzing the carbonylation level in $H_2O_2^-$ or cytokine cocktail–treated human islets in the presence of low glucose conditions. Histogram showing the intracellular carbonylation in untreated and stressed human islet cells from DNPH solution–treated cells (red) compared with the background intensity from non-DNPH–treated cells (black) for each individual sample, respectively. One representative experiment out of four human islet donor experiments is shown. *B*: The mean fluorescence intensity (MFI) of Alexa Fluor 488 (AF488) from DNPH solution–treated cells (red) compared with the background MFI from non-DNPH–treated cells in untreated and stressed human islet cells. Data were generated from four human islet donors and presented as mean with SE. The range of MFI for second Ab conjugated with AF488 control is 9.4 to 163. *C*: After 16.7 mmol/L glucose stimulation, islets were analyzed by confocal microscopy with triple immunofluorescence for insulin (red), P4Hb (blue), and carbonylation (green) with DNPH derivatization (bottom panel) or HCl background control (top panel). One representative experiment out of six human islet donor experiments is shown. *D–F*: Intact human islets were incubated with low or high glucose after treatment with H_2O_2 or cytokines. Supernatant was collected, and secretory insulin (*D*) or proinsulin (*E*) was measured by ELISA. The secretory proinsulin/insulin ratio from individual stressed human islets in the presence of low or high glucose was shown in *F*. Data were generated from six human islet donors and presented as means with SE (*D–F*). *$P < 0.05$.

stressed islets, we observed that protein carbonylation is increased in β-cells after glucose stimulation compared with untreated islets (increase in central green color compared with untreated islets in Fig. 2*C*, middle panel). Insulin synthesis and secretion are not increased under these conditions (blue-green merged cells in Fig. 2*C*). However, the greatest signal of carbonylated P4Hb colocalization with insulin in β-cells arises after glucose stimulation combined with cytokine-stressed islets (indicated as white in merged images in Fig. 2*C*, right panel).

Importantly, isolated human islets have impaired glucose-stimulated insulin secretion under oxidative or cytokine stress (Fig. 2*D*). From healthy human islets (n = 6), insulin release increased an average of 3.0 ± 1.6-fold between high (16.7 mmol/L) and low (5.5 mmol/L) glucose exposure. The insulin release was significantly reduced in H_2O_2 or inflammatory cytokines (IFN-γ, IL-1β, and TNF-α) treatment as compared with the untreated islets to 1.7 ± 0.6-fold in H_2O_2-treated islets and to 1.3 ± 0.8-fold in cytokine-treated islets. However, the secretory proinsulin level is disproportionately elevated in cytokine-treated islets compared with untreated islets with either low or high glucose exposure (Fig. 2*E*). Therefore, islets treated with cytokines significantly increase their ratio of proinsulin over insulin concentration in secretory content compared with untreated islets (Fig. 2*F*). These findings demonstrate that the increase in carbonylated P4Hb is coincident with disturbance of insulin biosynthesis and secretion in human pancreatic β-cells.

P4Hb Is Carbonylated Under Oxidative Stress in β-Cells and Is Immunoreactive to T1D Serum

Diabetic inflammation leads to oxidative stress, contributing to the progression of β-cell dysfunction. Treatment of

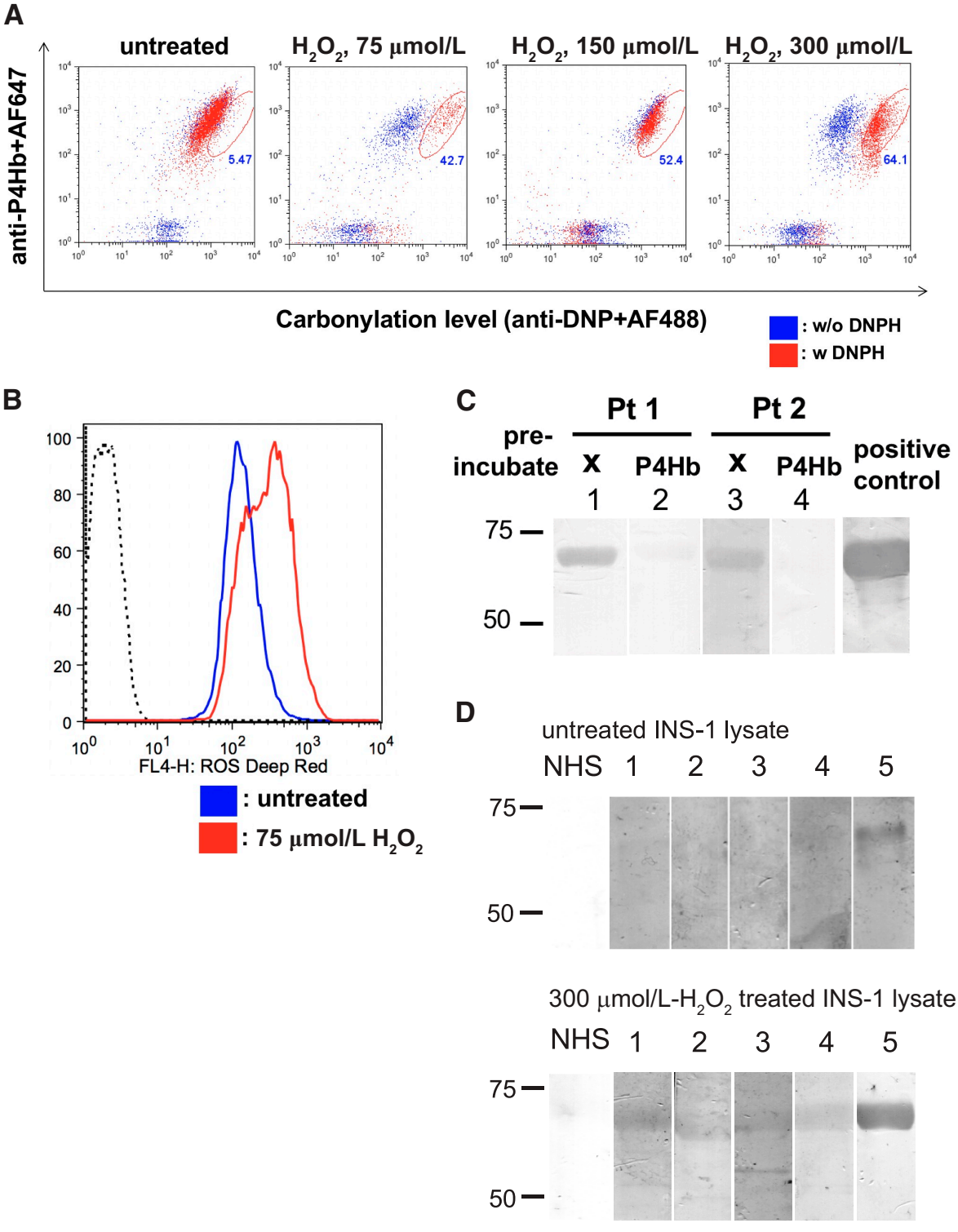

Figure 3—P4Hb is carbonylated under oxidative stress and is immunoreactive to T1D serum. INS-1 cells were treated with different concentrations of H_2O_2 for 1 h and analyzed for carbonylation by DNPH as described in *Research Design and Methods* (*A*) and ROS by Deep Red dye (*B*) by flow cytometry, respectively. Data are representative of two experiments; $n = 3$ for each experiment. *C*: The H_2O_2-treated (300 µmol/L) INS-1 lysate was separated by SDS-PAGE and transferred onto nitrocellulose membrane, followed by immunoblot with

rat β INS-1 cells with H_2O_2 increased the carbonylation content in a dose-dependent manner (Fig. 3*A*) due to an increase in ROS as a result of H_2O_2 exposure (Fig. 3*B*). Next, we used a 300 μmol/L H_2O_2-treated INS-1 cell lysate that contains appreciable quantities of intracellular carbonylated proteins (Fig. 3*A*) to probe the levels of immunoreactivity against carbonylated proteins within serum from patients with T1D. As shown in Fig. 3*C*, serum from patients with T1D recognized one protein band that has a similar polypeptide molecular weight as P4Hb (lanes 1 and 3). Preincubation of serum from patients with T1D with rhP4Hb inhibited binding to the presumed P4Hb band (lanes 2 and 4). However, serum from healthy donors did not have any immunoreactivity to either 300 μmol/L H_2O_2-treated or untreated INS-1 cell lysate (Fig. 3*D*, lane marked for normal human serum [NHS]). In addition, T1D serum has stronger immunoreactivity to 300 μmol/L H_2O_2-treated INS-1 cell lysate (Fig. 3*D*, bottom panel) compared with untreated INS-1 cell lysate (Fig. 3*D*, top panel). After treatment of INS-1 cells with IFN-γ plus IL-1β, cells will initially produce superoxide/peroxide and then will later generate nitric oxide (NO) (Supplementary Fig. 1*A*). NO synthase inhibitor (N^G-monomethyl-L-arginine) and ROS inhibitor (apocynin) were used to confirm that cytokine-triggered carbonylation of P4Hb in islet cells is mediated via ROS instead of NO. As shown in Supplementary Fig. 1*B*, H_2O_2- and cytokine-induced carbonylation was suppressed by N^G-monomethyl-L-arginine but not by apocynin.

Circulating Autoreactive Lymphocytes and Autoantibodies Against P4Hb in NOD and Patients With T1D

We next evaluated cellular and humoral immune responses to P4Hb over the course of disease development in NOD mice. Isolated pooled lymph node cells, including pancreatic lymph nodes from both prediabetic NOD and C57BL/6 mice, were stimulated with titrating concentrations of rhP4Hb protein. While control C57BL/6 mice showed little proliferative response to rhP4Hb, there is a clear dose-dependent proliferative response in prediabetic NOD mice (Supplementary Fig. 2*A*).

Solid-phase serum immunoassays demonstrate the anti-P4Hb IgG titer was significantly higher from 4–28-week-old NOD mice compared with 15–20-week-old BALB/c mice (Supplementary Fig. 2*B*). As shown in Supplementary Table 2, all diabetic NOD mice had anti-insulin IgG antibody and five of six mice had anti-P4Hb IgG antibody. In prediabetic NOD mice (n = 16), 14 mice had anti-P4Hb IgG antibody, while 6 mice had anti-insulin IgG antibody. Only 2 mice (of 22) lack antibody to either P4Hb or insulin. Our data indicate that anti-P4Hb antibodies arise early in disease and precede or arise coincidently with the onset of autoimmunity to insulin.

To assess T-cell responses to P4Hb in patients with T1D, we focused on residues 96–114, a segment of the protein that includes a potential carbonylation site (Thr101) and contains a predicted DRB1*04:01 binding motif (this allele is part of the high-risk DR4/DQ8 haplotype). After verifying HLA binding of the T101 peptide (Fig. 4*A*), we produced the corresponding HLA class II tetramer and used this as a tool to visualize T101-specific T-cell responses in 11 unique subjects with T1D. We observed tetramer staining that was significantly higher in magnitude (P = 0.0020) than background staining with a tetramer loaded with an irrelevant peptide (Fig. 4*B*). To ask whether carbonylation is required for immunogenicity, we isolated and expanded a T101-responsive T-cell clone and assessed its proliferation in response to carbonylated T101 or wild-type peptide. The clone proliferated robustly in response to the carbonylated T101 peptide (and this response was HLA-DR restricted), but failed to respond to the wild-type peptide (Fig. 4*C*). Given that the wild-type and T101 peptides bind with similar affinity to DRB1*04:01, T101 most likely functions as a required T-cell receptor (TCR) contact (Fig. 4*D*).

We next assessed P4Hb-specific antibody in patients with T1D. Patients with early-onset T1D (n = 21; <1 year of disease duration) have significantly higher anti-P4Hb IgG compared with healthy subjects (n = 10) (Fig. 4*E*). Moreover, the majority of patients with early-onset T1D (76%) have either anti-P4Hb alone (52%; 11 of 21 patients) or anti-P4Hb linked with anti-insulin (auto)antibodies (24%; 5 of 21 patients). Of interest, no serum from subjects with early-onset T1D had anti-insulin IgG (auto)antibodies without the presence of anti-P4Hb antibodies. In this set of patients with early-onset T1D, 8 of 21 patients had serum serially collected before and after insulin therapy (Table 2). Patients 1, 2, and 3 exhibited anti-P4Hb prior to the onset of anti-insulin antibodies (with patients 2 and 3 making anti-P4Hb prior to insulin therapy).

Serum autoantibodies against carbonylated rhP4Hb and its native counterpart in individuals with established T1D (n = 18; serum C-peptide <0.5 ng/mL) and healthy control subjects (n = 14) were also examined by ELISA. It is not surprising that most patients with established T1D develop insulin antibody after exogenous insulin therapy (Table 3). Most patients with established T1D maintained the detectable antibodies against either P4Hb and/or carbonylated P4Hb (12 of 18 patients). However, there is no statistical correlation between the presence of anti-P4Hb/

mouse polyclonal anti-P4Hb as positive control and sera from two patients with established T1D (Pt 1 and 2). Sera were preincubated with rhP4Hb before immunoblot as indicated. *D*: Immunoblot analysis for NHS and sera from five established patients with T1D (lanes 1–5) reactive to untreated INS-1 cell lysate (top panel) or 300 μmol/L H_2O_2-treated INS-1 lysate (bottom panel). AF488, Alexa Fluor 488; w, with; w/o, without.

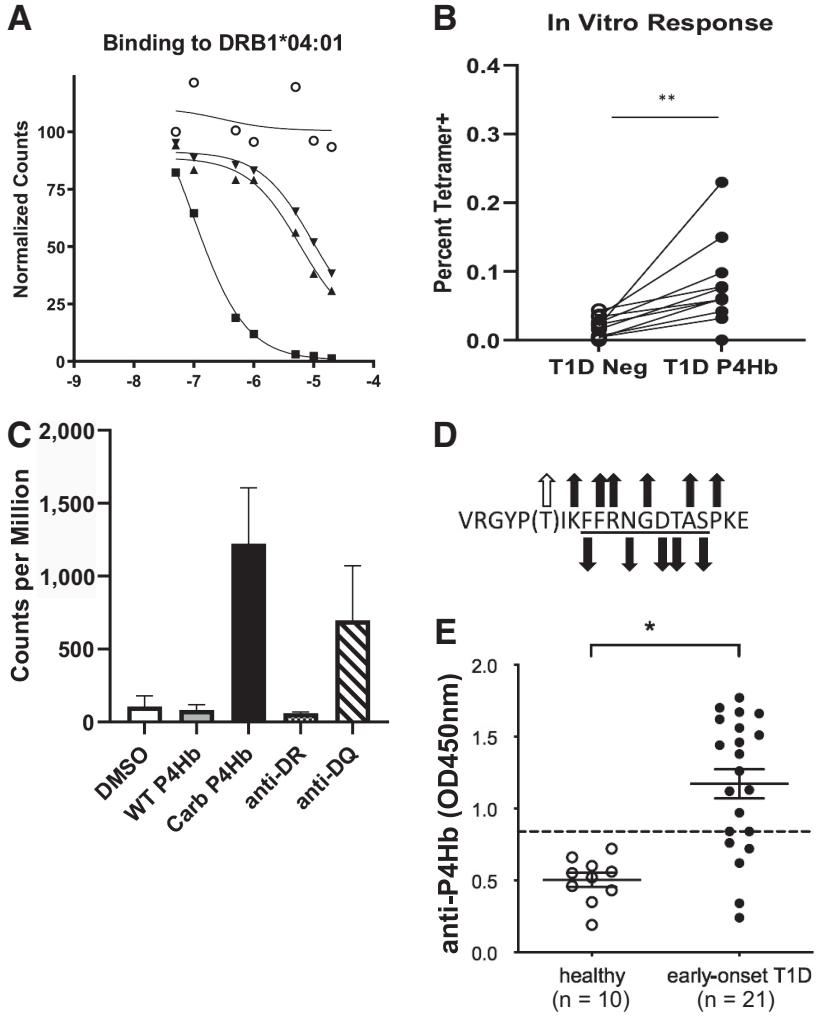

Figure 4—The circulating autoreactive T cells and IgG autoantibodies against P4Hb from patients with T1D. *A*: To assess potential T-cell recognition, we obtained a carbonylated peptide (synthesized by Mimotopes) with a predicted binding motif and containing a verified carbonylated residue (T101) and evaluated its ability to bind to recombinant DRB1*04:01 protein in a competition assay, observing detectable binding that was similar to a previously reported influenza epitope (a nonbinding GRP94 peptide is also shown as a reference condition). ▼, wild-type (WT) P4Hb; ▲, carboylated (Carb) T101-P4Hb; ■, HA306; ●, GRP94 D620. *B*: T cells that recognize the carbonylated P4Hb peptide were expanded from the PBMCs of 11 unique subjects with T1D and detected by HLA class II tetramer staining. Observed responses were modest, but significantly higher in magnitude (**P = 0.0039, Wilcoxon matched-pairs signed rank test) than background staining. *C*: We further confirmed T-cell recognition of the carbonylated peptide by sorting a responsive T-cell clone. This clone exhibited significantly higher proliferation (based on [^{3}H]thymidine incorporation) in response to 10 μg/mL of its cognate peptide as compared with mock stimulation with DMSO (P = 0.0194, unpaired t test). *D*: The peptide has a strong DRB1*04:01 binding motif (underlined) with favorable residues in the major HLA binding pockets (downward-facing arrows). Possible TCR contact residues (upward-facing arrows) include small, minimally interfacing amino acids and a constrained proline at the C terminus of the peptide but larger residues at the N terminus, suggesting biased N-terminal T-cell docking and possible involvement of carbonylated T101 as an auxiliary T-cell contact. *E*: The serum levels of anti-rhP4Hb from patients with early-onset T1D (n = 21) and healthy control subjects (n = 10) were measured by ELISA. Data were mean ± SE with the number of human samples indicated at the bottom of each group. Cutoff line is shown as a dotted line and is defined as the value of average OD_{405nm} + 2 SD from healthy individuals. *$P < 0.001$, Student t test. Neg, negative.

carbonylated P4Hb and other established autoantibodies including anti-GAD65, anti-IA2, and anti-ZnT8.

Identification of Carbonyl Residues in Human P4Hb

To map the potential carbonylation sites, rhP4Hb was in vitro carbonylated by oxidative Fenton reaction (27). The carbonyl modification of oxidative rhP4Hb was confirmed with OxyBlot as previously described (Supplementary Fig. 3). By using the computational tool, PTIK, aa 100–103, in human P4Hb (hP4Hb) protein is the sole predicted carbonylation region by carbonylated sites and protein detection as described (28). Of interest, T101 is the same residue we

Table 2—Anti-P4Hb and anti-INS autoantibodies in serial serum samples from patients with early-onset T1D

	Patient 1		Patient 2		Patient 3		Patient 4		Patient 5		Patient 6		Patient 7		Patient 8	
	Anti-P4Hb	Anti-INS	Anti-P4Hb	Anti-INS	Anti-P4Hb	Anti-INS	Anti-P4Hb	Anti-INS	Anti-P4Hb	Anti-INS	Anti-P4Hb	Anti-INS	Anti-P4Hb	Anti-INS	Anti-P4Hb	Anti-INS
Before INS therapy	–	–	+	–	+	–	–	–	–	–	–	–	–	–	+	–
After INS therapy (months)																
1	n.s.	n.s.	n.s.	n.s.	+	–	–	–	+	+	n.s.	n.s.	n.s.	n.s.	n.s.	n.s.
3	+	–	+	–	+	+	n.s.	n.s.	n.s.	n.s.	n.s.	n.s.	n.s.	n.s.	n.s.	n.s.
6	n.s.	n.s.	n.s.	n.s.	n.s.	n.s.	n.s.	n.s.	n.s.	n.s.	n.s.	n.s.	–	–	–	–
9	n.s.	n.s.	+	+	n.s.	n.s.	n.s.	n.s.	n.s.	n.s.	+	–	n.s.	n.s.	n.s.	n.s.
12	+	+	+	+	n.s.	n.s.	n.s.	n.s.	+	–	n.s.	n.s.	n.s.	n.s.	–	–

+, present; –, absent; n.s., no sample collected.

identified as above as a potential TCR contact amino acid. Besides T101, we identified five more carbonylation sites in oxidative rhP4Hb by DNPH-assisted MS. Of note, one carbonylation site (K31) in the catalytic domain was identified in both control and oxidative rhP4Hb. In total, six carbonylation sites were identified in oxidative rhP4Hb, including three residues in catalytic sites and three residues in the noncatalytic/substrate binding domain (Fig. 5*A*). One representative MS/MS spectra of carbonyl-P4Hb peptide is shown in Fig. 5*B* (the details of LC-MS/MS data are summarized in Supplementary Table 3).

Human PDI (hPDI) is a redox-regulated chaperone responsible for catalyzing the folding of secretory proteins. The crystal structures of yeast and hPDI in different redox states showed that four thioredox domains (a, b, b', and a') are arranged as a horseshoe shape with the CXXC active sites, in domain a and a', facing each other (29,30). The b' domain of mammalian PDI has been mapped as the primary substrate binding site (31). Compared with the reduced state of hPDI, the oxidized hPDI results in open conformation with more extended hydrophobic areas for its substrate binding (32). The six carbonyl residues identified in this work are also highlighted in the three-dimensional structure of hP4Hb protein (Fig. 5*C*).

DISCUSSION

The overall aim of this study was to develop and use a broad, proteomics-based screen to identify posttranslationally modified proteins and evaluate both autoimmunity and their contributions to pathways of proinsulin and insulin production. The clinical and biological relevance of this work is bolstered by other studies that demonstrate critical protein modifications in the induction and diagnosis of autoimmunity (33,34). For example, citrullination is a product of the deamination of arginine residues and a hallmark PTM in diagnostics and the severity of rheumatoid arthritis (35). Moreover, protein citrullination and antibodies against citrullinated self-proteins have also played an important role in T1D (36,37).

T1D pathogenesis is linked to the generation of tissue free radicals (38). Carbonylation is the major PTM product in tissues/cells under oxidative stress. Oxidation-triggered PTMs result in increased carbonyl-modified plasma proteins in patients with T1D (39). Moreover, hyperglycemia amplifies oxidative stress, leading to pancreatic β-cell and endothelial cell dysfunction (40). The deficiency of glutathione peroxidase 1, a major antioxidant enzyme, leads to metabolic changes similar to T1D. Carbonylation results in enzymatic inactivation of glutathione peroxidase 1, which might contribute to insulin resistance (41).

One novel autoantigen identified in this study, P4Hb (PDIA1), is a member of the PDI family and the β subunit of a tetramer of P4H. This tetramer holoenzyme has several important cellular functions, including the hydroxylation of proline residues in procollagen. Recently, we

Table 3—Autoantibody panel in patients with established T1D

Patient number[a]	Sex	Age at draw (years)	Disease duration (years)	Anti-INS[b]	Anti-GAD65[b]	Anti-IA2[b]	Anti-ZnT8[b]	Anti-P4Hb[c]	Anti-carbonyl P4Hb[c]
1	Male	46	41.9	+	+	–	–	–	–
2	Male	46	32.1	+	+	–	–	–	–
3	n.k.	16	5.2	+	+	+	+	–	–
4	n.k.	10	6.5	+	–	–	–	+	+
5	Female	11	10	+	–	+	–	+	+
6	Female	70	14.5	+	–	–	–	+	+
7	Male	17	7.8	+	+	+	–	+	+
8	n.k.	9	5.4	+	–	–	–	+	+
9	Female	59	55	+	–	–	–	–	+
10	Female	13	3.6	+	+	+	+	+	+
11	n.k.	14	10.3	+	–	–	–	+	+
12	Female	45	42.6	+	+	+	–	+	+
13	Male	6	4.3	+	+	–	–	+	+
14	Male	12	2.7	+	+	–	–	–	–
15	Female	11	4.1	+	–	–	–	–	–
16	Male	14	9.4	+	+	+	–	+	+
17	Female	19	5.6	+	+	+	+	+	+
18	Male	40	26.9	–	–	–	–	–	–
Mean (n = 18)		25.44	15.99						
SD (n = 18)		19.22	16.26						

n.k., not known. [a]All patients with T1D with serum C-peptide <0.5 ng/mL. [b]The presence (+) or absence (–) of autoantibodies against to INS, GAD65, IA2, and ZnT8 were determined by the Barbara Davis Center Autoantibody/HLA Service Center using standardized radioimmunoassay. [c]Defined as positive if ELISA optical density (OD) was higher than that of healthy individuals (average OD + 2 SD). Healthy control subjects (n = 14); age: 37.84 + 11.76 years; sex: 7 male, 6 female, and 1 not known.

found that P4Hb plasma levels were increased in prediabetic NOD mice and the serum of children with recent-onset T1D compared with age- and sex-matched control subjects without diabetes (42). Relevant to the biology of T1D, P4Hb activity in β-cells modulates glucose-stimulated release of insulin (26). P4Hb is both a chaperone and thioreductase, participating in disulfide bond formation and isomerization during the process of insulin biosynthesis and secretion. It has been demonstrated that chemical modification of PDI, ablating the thioredoxin activity, prevents the refolding of denatured and reduced proinsulin in vitro (43). Moreover, proinsulin forms aggregates in the absence of the chaperone activity of the PDI. Our data are consistent with recent studies illustrating that pancreatic β-cells fail to properly process proinsulin in early-onset T1D (44).

The significance of P4Hb-associated insulin misfolding is illustrated in studies from the Akita mouse model, in which improper disulfide bond formation leads to the retention of misfolded proinsulin in the β-cell ER (45,46). Others have proposed that restoration of the unfolded protein response in pancreatic β-cells protects mice against T1D (47). Moreover, GRP78/BiP, one of the carbonyl-modified antigenic islet proteins identified in this study, is also an ER chaperone. The transcriptional activity of GRP78/BiP promoter is upregulated in response to unfolded proteins in the ER (48). Of interest, the mispairing of disulfide bonds in proinsulin increases ER stress response, resulting in GRP78/BiP promoter activation in INS-1 β-cells (49). In this study, our data demonstrated that carbonylation of P4Hb is greatly increased in human islets under oxidative or inflammatory cytokine stress. Moreover, insulin production is significantly reduced in stressed human islets compared with untreated human islets, coincident with carbonyl modification of P4Hb. Recently, antibodies against oxidized insulin were detected in patients with T1D (50). P4Hb, but also insulin itself, may undergo carbonylation in pancreatic islets during insulitis and results in misfolded proinsulin or insulin, a potential initiating event leading to the onset of T1D. This pathway explains observations of increasing proinsulin/insulin ratios in the progression of T1D as recently reported (11,44).

In conclusion, we identified selected inflammation-induced carbonyl protein modifications from both mouse and human pancreatic islets. These modifications may

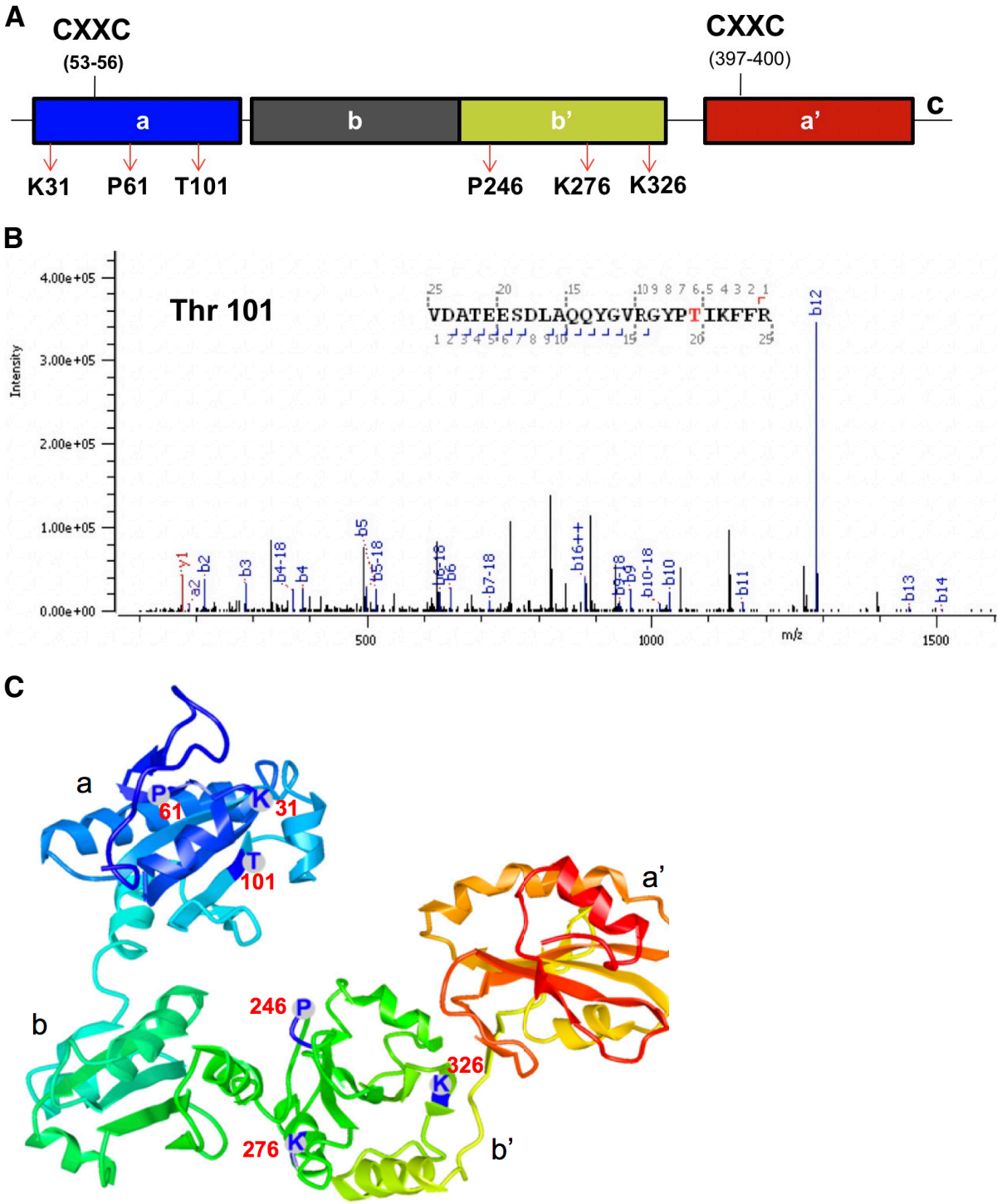

Figure 5—Carbonylation modifications in hP4Hb (Protein Data Bank 4EKZ). *A*: The locations of carbonyl residue of hP4Hb that arose during in vitro oxidation are indicated in the functional domains, respectively. P4Hb is composed of four thioredoxin-like domains *abb'a'* and one C-terminal acidic tail, where *a* and *a'* stand for catalytic domain with CXXC motif and b and *b'* stand for noncatalytic domain. The *b'* domain also contains the substrate binding site. The residual numbering is for hP4Hb with signal sequence. *B*: Representative MS/MS spectra of DNPH-derivatized peptide out of seven peptides identified in oxidative rhP4Hb is shown. The data emphasize identification of carbonyl modification of Thr101 of P4Hb, found as a T-cell determinant site in Fig. 4. *C*: The carbonylation sites of K31, P61, and T101 in *domain a* and P246, K276, and K326 in *domain b'* are indicated in the hP4Hb structure.

lead to a specific loss of both β- and T-cell immune tolerance. This approach successfully identified both novel and known T1D autoantigens, such as GRP78 and pancreatic amylase. Anti-P4Hb autoimmunity generally precedes anti-insulin autoantibodies and β-cell dysfunction in T1D. This autoimmune pathway is marked by impaired glucose-stimulated insulin secretion and provides an explanation for increased proinsulin/insulin ratios found during the progression of human T1D. Beyond identifying novel autoimmune targets of early T1D and altered mechanisms of insulin metabolism, these studies also provide potential antioxidant therapeutic strategies to reverse disease-relevant biochemical pathways, such as carbonyl modification.

Acknowledgments. The authors thank Prof. Colin Thorpe (University of Delaware, Newark, DE) for providing the human hPDI-pTrcHisA clone for these studies; Cameron Gesick, Elaina Bruck, Emily Schroeder, and Tyler Masters (members of the Mamula laboratory) for excellent technical assistance for this study; Ningwen Tai (L. Wen Laboratory, Yale University School of Medicine, New Haven, CT) for technical assistance in isolation of pancreatic islets; Lucy Zhang (L. Wen Laboratory, Yale University School of Medicine, New Haven, CT) for careful management of the NOD mouse colony; Drs. Carla Greenbaum and Jane Buckner (Benaroya Research Institute, Virgina Mason Medical Center, Seattle, WA) for collecting and archiving human samples for this work; and Navin Rauniyar (W.M. Keck Foundation Biotechnology Resource Laboratory, Yale University) for the expertise in high-resolution MS.

Funding. This research was supported by the Diabetes Research Foundation Training Program in Investigative Rheumatology (5T32-AR007107 to S.E.C.), an Innovative Grant from JDRF (1-INO-2022-1116-A-N to M.J.M.), and a National Institutes of Health grant (DK104205-01 to K.C.H. and M.J.M.). L.W. was supported by National Institutes of Health grant DK092882 and the Diabetes Research Center (DK-11-015).

Duality of Interest. No potential conflicts of interest relevant to this article were reported.

Author Contributions. M.-L.Y. designed and performed the experimentation, data analysis, and composition of the manuscript. S.E.C., R.G., and P.G. performed the experimentation of 2D gel electrophoresis, confocal microscopy, and tetramer analysis of human T cells, respectively. K.C.H. and M.J.M. directed the project and edited the manuscript. C.S. and K.C.H. provided key T1D serum sets to the study. J.P. and L.W. provided the NOD mice used in the study and supervised pancreatic islet isolation. T.T.L. and J.K. performed LC-MS/MS and analyzed high-resolution mass spectrometry data. F.S., H.M.T., S.G.C., C.F.C., E.A.J., C.S., C.E.-M., and L.W. provided helpful discussion and manuscript edits. M.J.M. is the guarantor of this work and, as such, had full access to all of the data in the study and takes responsibility for the integrity of the data and the accuracy of the data analysis.

Prior Presentation. Parts of this study were presented in abstract form at the 100th Annual Meeting of American Association of Immunologists (IMMUNOLOGY 2016), Seattle, WA, 13–17 May 2016, and the 5th European Congress of Immunology, Amsterdam, the Netherlands, 2–5 September 2018.

References

1. Yang ML, Doyle HA, Clarke SG, Herold KC, Mamula MJ. Oxidative modifications in tissue pathology and autoimmune disease. Antioxid Redox Signal 2018;29:1415–1431

2. Newsholme P, Keane KN, Carlessi R, Cruzat V. Oxidative stress pathways in pancreatic β-cells and insulin-sensitive cells and tissues: importance to cell metabolism, function, and dysfunction. Am J Physiol Cell Physiol 2019;317:C420–C433

3. Trigwell SM, Radford PM, Page SR, et al. Islet glutamic acid decarboxylase modified by reactive oxygen species is recognized by antibodies from patients with type 1 diabetes mellitus. Clin Exp Immunol 2001;126:242–249

4. Piganelli JD, Flores SC, Cruz C, et al. A metalloporphyrin-based superoxide dismutase mimic inhibits adoptive transfer of autoimmune diabetes by a diabetogenic T-cell clone. Diabetes 2002;51:347–355

5. Stosic-Grujicic SD, Miljkovic DM, Cvetkovic ID, Maksimovic-Ivanic DD, Trajkovic V. Immunosuppressive and anti-inflammatory action of antioxidants in rat autoimmune diabetes. J Autoimmun 2004;22:267–276

6. Fedorova M, Bollineni RC, Hoffmann R. Protein carbonylation as a major hallmark of oxidative damage: update of analytical strategies. Mass Spectrom Rev 2014;33:79–97

7. Frohnert BI, Bernlohr DA. Protein carbonylation, mitochondrial dysfunction, and insulin resistance. Adv Nutr 2013;4:157–163

8. Shao CH, Capek HL, Patel KP, et al. Carbonylation contributes to SERCA2a activity loss and diastolic dysfunction in a rat model of type 1 diabetes. Diabetes 2011;60:947–959

9. Rameshthangam P, Srinivasan P, Arulvasu C, Gowdhaman D, Neeraja P. Protein carbonylation as biomarker(s) in serum patients with type 2 diabetes. J Pharm Res 2011;4:348–351

10. Jang I, Pottekat A, Poothong J, et al. PDIA1/P4HB is required for efficient proinsulin maturation and ß cell health in response to diet induced obesity. eLife 2019;8:e44528

11. Sims EK, Bahnson HT, Nyalwidhe J, et al.; T1D Exchange Residual C-peptide Study Group. Proinsulin secretion is a persistent feature of type 1 diabetes. Diabetes Care 2019;42:258–264

12. Alcazar O, Buchwald P. Concentration-dependency and time profile of insulin secretion: dynamic perifusion studies with human and murine islets. Front Endocrinol (Lausanne) 2019;10:680

13. Bollineni RCh, Hoffmann R, Fedorova M. Identification of protein carbonylation sites by two-dimensional liquid chromatography in combination with MALDI- and ESI-MS. J Proteomics 2011;74:2338–2350

14. Linares M, Marín-Garcíía P, Méndez D, Puyet A, Diez A, Bautista JM. Proteomic approaches to identifying carbonylated proteins in brain tissue. J Proteome Res 2011;10:1719–1727

15. Matallana-Surget S, Cavicchioli R, Fauconnier C, et al. Shotgun redox proteomics: identification and quantitation of carbonylated proteins in the UVB-resistant marine bacterium, Photobacterium angustum S14. PLoS One 2013;8:e68112

16. Guo J, Prokai L. To tag or not to tag: a comparative evaluation of immunoaffinity-labeling and tandem mass spectrometry for the identification and localization of posttranslational protein carbonylation by 4-hydroxy-2-nonenal, an end-product of lipid peroxidation. J Proteomics 2011;74:2360–2369

17. Farasyn T, Crowe A, Hatley O, et al. Preincubation with everolimus and sirolimus reduces organic anion-transporting polypeptide (OATP)1B1- and 1B3-mediated transport independently of mTOR kinase inhibition: implication in assessing OATP1B1- and OATP1B3-mediated drug-drug interactions. J Pharm Sci 2019;108:3443–3456

18. Strollo R, Vinci C, Napoli N, Pozzilli P, Ludvigsson J, Nissim A. Antibodies to post-translationally modified insulin as a novel biomarker for prediction of type 1 diabetes in children. Diabetologia 2017;60:1467–1474

19. Gebe JA, Novak EJ, Kwok WW, Farr AG, Nepom GT, Buckner JH. T cell selection and differential activation on structurally related HLA-DR4 ligands. J Immunol 2001;167:3250–3256

20. Ettinger RA, Papadopoulos GK, Moustakas AK, Nepom GT, Kwok WW. Allelic variation in key peptide-binding pockets discriminates between closely related diabetes-protective and diabetes-susceptible HLA-DQB1*06 alleles. J Immunol 2006;176:1988–1998

21. Ise W, Kohyama M, Nutsch KM, et al. CTLA-4 suppresses the pathogenicity of self antigen-specific T cells by cell-intrinsic and cell-extrinsic mechanisms. Nat Immunol 2010;11:129–135

22. Rondas D, Crèvecoeur I, D'Hertog W, et al. Citrullinated glucose-regulated protein 78 is an autoantigen in type 1 diabetes. Diabetes 2015;64:573–586
23. Buitinga M, Callebaut A, Marques Câmara Sodré F, et al. Inflammation-induced citrullinated glucose-regulated protein 78 elicits immune responses in human type 1 diabetes. Diabetes 2018;67:2337–2348
24. Endo T, Takizawa S, Tanaka S, et al. Amylase alpha-2A autoantibodies: novel marker of autoimmune pancreatitis and fulminant type 1 diabetes. Diabetes 2009;58:732–737
25. Winter WE, Schatz DA. Autoimmune markers in diabetes. Clin Chem 2011;57:168–175
26. Rajpal G, Schuiki I, Liu M, Volchuk A, Arvan P. Action of protein disulfide isomerase on proinsulin exit from endoplasmic reticulum of pancreatic β-cells. J Biol Chem 2012;287:43–47
27. Wondrak GT, Cervantes-Laurean D, Jacobson EL, Jacobson MK. Histone carbonylation in vivo and in vitro. Biochem J 2000;351:769–777
28. Maisonneuve E, Ducret A, Khoueiry P, et al. Rules governing selective protein carbonylation. PLoS One 2009;4:e7269
29. Wang C, Li W, Ren J, et al. Structural insights into the redox-regulated dynamic conformations of human protein disulfide isomerase. Antioxid Redox Signal 2013;19:36–45
30. Tian G, Xiang S, Noiva R, Lennarz WJ, Schindelin H. The crystal structure of yeast protein disulfide isomerase suggests cooperativity between its active sites. Cell 2006;124:61–73
31. Klappa P, Ruddock LW, Darby NJ, Freedman RB. The b′ domain provides the principal peptide-binding site of protein disulfide isomerase but all domains contribute to binding of misfolded proteins. EMBO J 1998;17:927–935
32. Wang C, Yu J, Huo L, Wang L, Feng W, Wang CC. Human protein-disulfide isomerase is a redox-regulated chaperone activated by oxidation of domain a′. J Biol Chem 2012;287:1139–1149
33. McGinty JW, Marré ML, Bajzik V, Piganelli JD, James EA. T cell epitopes and post-translationally modified epitopes in type 1 diabetes. Curr Diab Rep 2015;15:90
34. McLaughlin RJ, Spindler MP, van Lummel M, Roep BO. Where, how, and when: positioning posttranslational modification within type 1 diabetes pathogenesis. Curr Diab Rep 2016;16:63
35. Zendman AJ, Vossenaar ER, van Venrooij WJ. Autoantibodies to citrullinated (poly)peptides: a key diagnostic and prognostic marker for rheumatoid arthritis. Autoimmunity 2004;37:295–299
36. Yang ML, Sodré FMC, Mamula MJ, Overbergh L. Citrullination and PAD enzyme biology in type 1 diabetes - regulators of inflammation, autoimmunity, and pathology. Front Immunol 2021;12:678953
37. Yang ML, Horstman S, Gee R, et al. Citrullination of glucokinase is linked to autoimmune diabetes. Nat Commun 2022;13:1870
38. Bashan N, Kovsan J, Kachko I, Ovadia H, Rudich A. Positive and negative regulation of insulin signaling by reactive oxygen and nitrogen species. Physiol Rev 2009;89:27–71
39. Cakatay U, Telci A, Salman S, Satman L, Sivas A. Oxidative protein damage in type I diabetic patients with and without complications. Endocr Res 2000;26:365–379
40. Patel H, Chen J, Das KC, Kavdia M. Hyperglycemia induces differential change in oxidative stress at gene expression and functional levels in HUVEC and HMVEC. Cardiovasc Diabetol 2013;12:142
41. Hecker M, Wagner AH. Role of protein carbonylation in diabetes. J Inherit Metab Dis 2018;41:29–38
42. Syed F, Singhal D, Raedschelders K, et al. A discovery-based proteomics approach identifies protein disulfide isomerase (PDIA1) as a biomarker of β cell stress in type 1 diabetes. 23 December 2021 [preprint]. bioRxiv: 10.1101/2021.12.22.473924
43. Winter J, Klappa P, Freedman RB, Lilie H, Rudolph R. Catalytic activity and chaperone function of human protein-disulfide isomerase are required for the efficient refolding of proinsulin. J Biol Chem 2002;277:310–317
44. Rodriguez-Calvo T, Zapardiel-Gonzalo J, Amirian N, et al. Increase in pancreatic proinsulin and preservation of β-cell mass in autoantibody-positive donors prior to type 1 diabetes onset. Diabetes 2017;66:1334–1345
45. Liu M, Hodish I, Rhodes CJ, Arvan P. Proinsulin maturation, misfolding, and proteotoxicity. Proc Natl Acad Sci USA 2007;104:15841–15846
46. Oyadomari S, Koizumi A, Takeda K, et al. Targeted disruption of the Chop gene delays endoplasmic reticulum stress-mediated diabetes. J Clin Invest 2002;109:525–532
47. Engin F, Yermalovich A, Nguyen T, et al. Restoration of the unfolded protein response in pancreatic β cells protects mice against type 1 diabetes [published correction appears in Sci Transl Med 2013;5:214er11]. Sci Transl Med 2013;5:211ra156
48. Tirasophon W, Welihinda AA, Kaufman RJ. A stress response pathway from the endoplasmic reticulum to the nucleus requires a novel bifunctional protein kinase/endoribonuclease (Ire1p) in mammalian cells. Genes Dev 1998;12:1812–1824
49. Haataja L, Manickam N, Soliman A, Tsai B, Liu M, Arvan P. Disulfide mispairing during proinsulin folding in the endoplasmic reticulum. Diabetes 2016;65:1050–1060
50. Strollo R, Vinci C, Arshad MH, et al. Antibodies to post-translationally modified insulin in type 1 diabetes. Diabetologia 2015;58:2851–2860

Supplemental Material

Supplementary Table 1. DRB1*04:01 subjects with established type 1 diabetes for T cell assays.

Patient	Gender	Age at draw (yrs)	Disease duration (yrs)
#1	female	43	6
#2	male	21	6
#3	female	34	7
#4	female	20	8
#5	male	20	5
#6	female	18	4
#7	male	18	7
#8	female	18	6
#9	male	19	6
#10	female	26	7
#11	female	51	38
	mean (n=11)	26.18	9.09
	SD (n=11)	11.47	9.64

Supplementary Table 2. Autoantibodies against P4Hb are present prior to the presence of anti-insulin and hyperglycemia in NOD mice.

NOD mice	age (weeks old, wks)	blood glucose ^ (blood glucose, mg/dL)	anti-P4Hb *	anti-insulin *
#1	4	− (123)	+	-
#2	4	− (138)	+	-
#3	4	− (180)	+	-
#4	4	− (204)	+	-
#5	4	− (88)	-	-
#6	4	− (194)	-	-
#7	8	− (104)	+	+
#8	8	− (96)	+	+
#9	8	− (93)	+	-
#10	8	− (159)	+	-
#11	8	− (116)	+	-
#12	8	− (99)	+	+
#13	11	− (60)	+	+
#14	11	− (178)	+	+
#15	28	− (113)	+	-
#16	28	− (167)	+	+
#17	20	+ (>500)	+	+
#18	22	+ (466)	+	+
#19	22	+ (>500)	+	+
#20	24	+ (363)	+	+
#21	26	+ (>500)	-	+
#22	28	+ (>500)	+	+

^, diabetics defined as positive if blood glucose concentration > 250 mg/dL

*, defined as positive if ELISA OD > (average OD + 2SD) of control mice (n=5)

Supplementary Table 3.
The carbonyl residues identified in human P4Hb under oxidative stress.

Domain in P4Hb	Position	Sequence	Modifications (variable)	PEP 2D	PEP 1D	|Log Prob|	Score	Delta Score	Delta Score	Modification	z	Observation m/z	ppm err.	Observation MH	Calculation MH
	DNPH derivitization before trypsin treatment														
a	Thr 101	K.VDATEESDLAQQYGVRGYPT[+178.01000]IKFFR.N	T20(Thr-DNPH / 178.01)	0.0075	0.0097	2.12	351.4	351.4	26.1		3	1023.4897	2.52	3068.4547	3068.447
b'	Lys 276	K.SVSDYDGKLSNFK[+179.02000]TAAESFK.G	K13(Lys-DNPH / 179.02)	0.0051	0.0065	2.29	339	339	27.9		3	792.0274	-1.09	2374.0676	2374.0702
b'	Lys 326	R.LITLEEEMTK[+179.02000]YKPESEELTAER.I	K10(Lys-DNPH / 179.02)	0.0036	0.0046	2.44	329.6	329.6	153.3		3	945.4476	0.51	2834.3283	2834.3269
	2nd time DNPH derivitization after trypsin treatment														
a	Lys 31**	R.K[+181.037]SNFAEALAAHK.Y	K1(Lys-DNPHred / 181.037)*	1.30E-06	2.20E-06	5.87	477.7	477.7	477.7		3	490.244	7.97	1468.7175	1468.7058
a	Pro 61	K.ALAP[+196.023]EYAK.A	P4(Lys-DNPHred / 196.023)*	1.80E-05	2.80E-05	4.75	355.6	326.5	326.5		2	529.749	0.04	1058.490	1058.490
b'	Pro 246	K.HNQLPLVIEFTEQTAP[+196.126]K.I	P16(Pro-DNPHred /196.12)*	1.50E-08	2.40E-08	7.82	444.3	444.3	376		3	781.4	0.29	2342.207	2342.206
b'	Lys 326	R.LITLEEEMTK[+179.021]YKPESEELTAER.I	K10(Lys-DNPH / 179.02)	8.10E-07	1.30E-06	6.09	383.2	383.2	187.8		3	945.4476	0.09	2834.333	2834.328

*DNPHred: DNPH + stabilizer
** K31was also identified in control rhP4Hb protein.

A

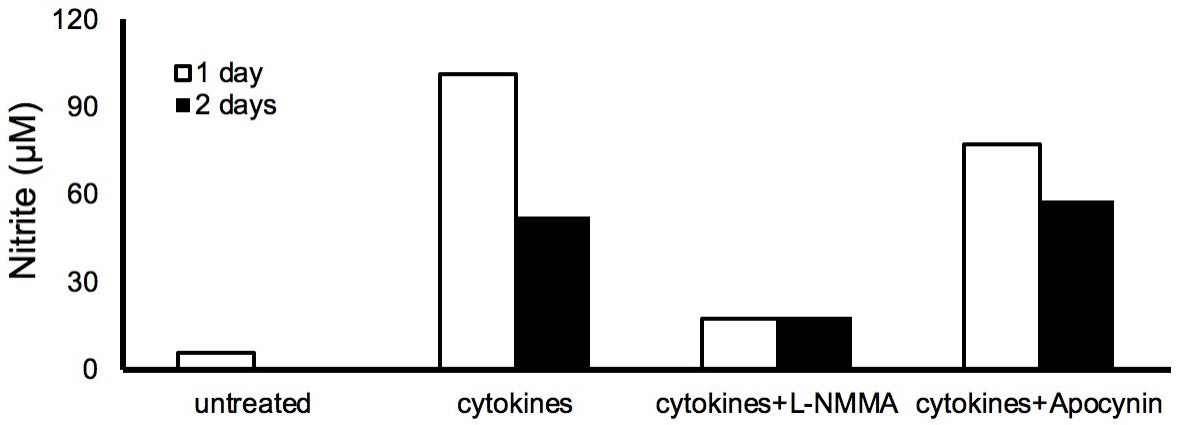

B

H_2O_2	-	+	+	+	-	-	-
cytokines	-	-	-	-	+	+	+
L-NMMA	-	-	+	-	-	+	-
apocynin	-	-	-	+	-	-	+

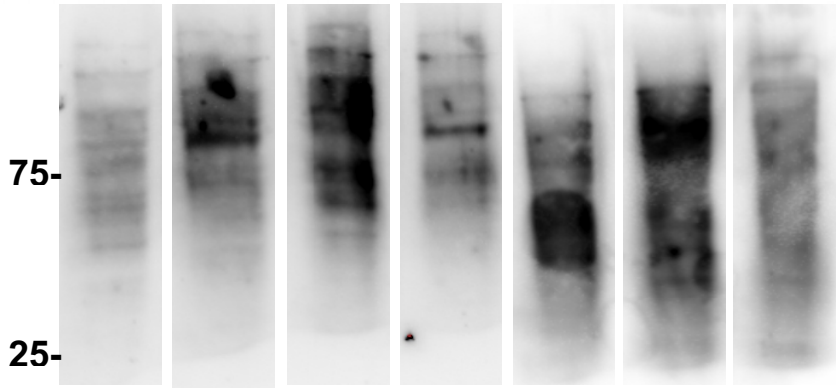

Supplementary Figure 1: The carbonylation triggered by H_2O_2 and cytokines in beta cells is mediated via reactive oxygen species (ROS) not nitrite. *A*: INS-1 cells were treated with cytokines (IFNγ+IL-1β) in the presence of L-NMMA (2mM) or apocynin (50μM). After one day or two days treatment, supernatant was collected and measured the nitrite level by using Griess reagent. *B*: The carbonylation level was measured by OxyBlot in untreated, 300 μM H_2O_2 (one hour) and cytokines treated (one day) INS-1 cells. Ten μg cell lysate protein were loading per lane. Molecular mass, in kDa, is indicated on the left.

A

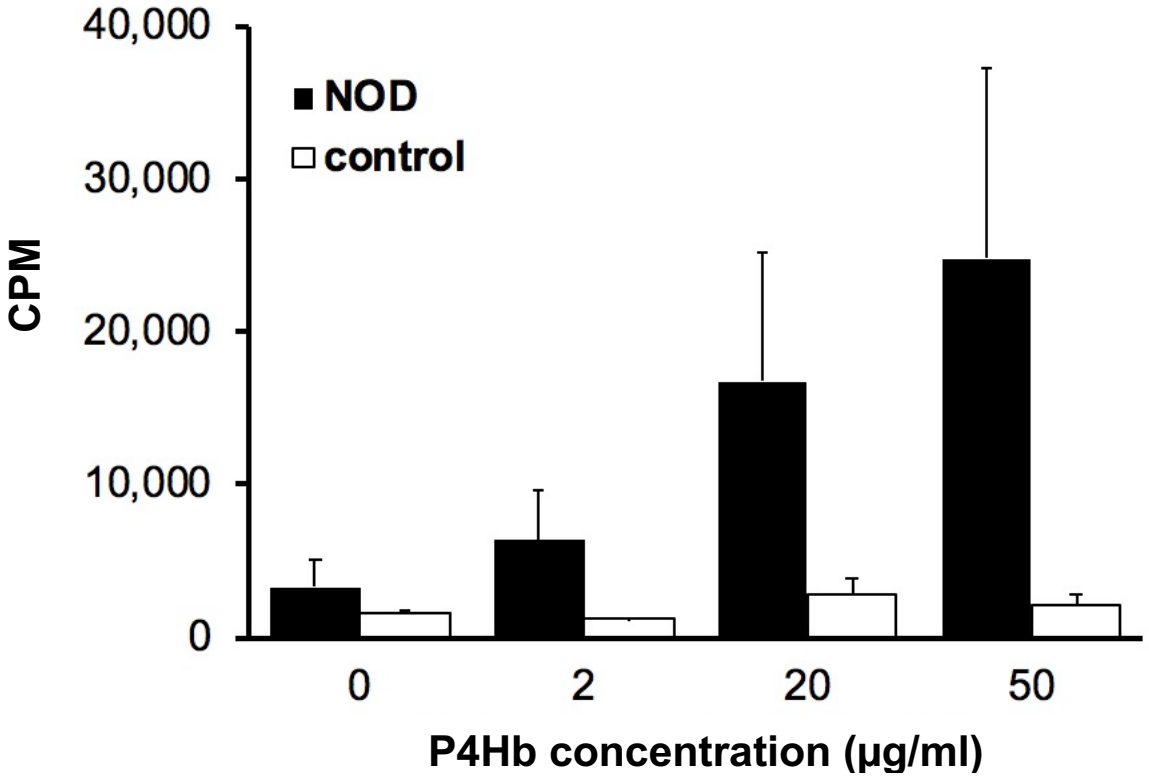
40,000
30,000
20,000
10,000
0
CPM
NOD
control
0
2
20
50
P4Hb concentration (µg/ml)

B

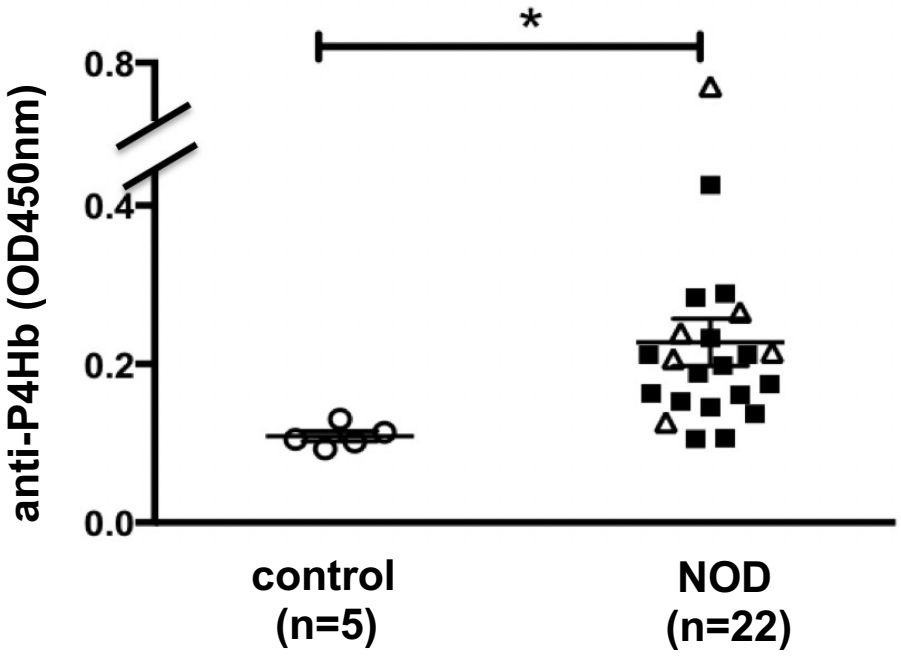
*
0.8
0.4
0.2
0.0
anti-P4Hb (OD450nm)
control
(n=5)
NOD
(n=22)

Supplementary Figure 2: The circulating autoreactive lymphocytes and IgG autoantibodies against P4Hb protein in NOD mice. *A*: Fresh pooled axillary, inguinal, brachial, popliteal and pancreatic lymph node cells (5×10^5) from 4- to 5-wk-old prediabetic NOD mice or control mice (C57Bl/6 strain) were plated with pre-coated anti-CD3 (10µg/ml) mAb as positive control or incubated with varying concentrations of recombinant human P4Hb (rhP4Hb) for 48 h. Then proliferation was measured by [3H]thymidine incorporation. *B*: The serum levels of anti-rhP4Hb in NOD and control mice (BALB/c strain) were measured by ELISA. The number of mice analyzed is indicated at the bottom of each group. *Student t test, $p<0.001$. The filled squares show data where the blood glucose content was less than 250 mg/dL; the open triangles data where the blood glucose was greater than 250 mg/dL. Error bars indicate SEM of mean.

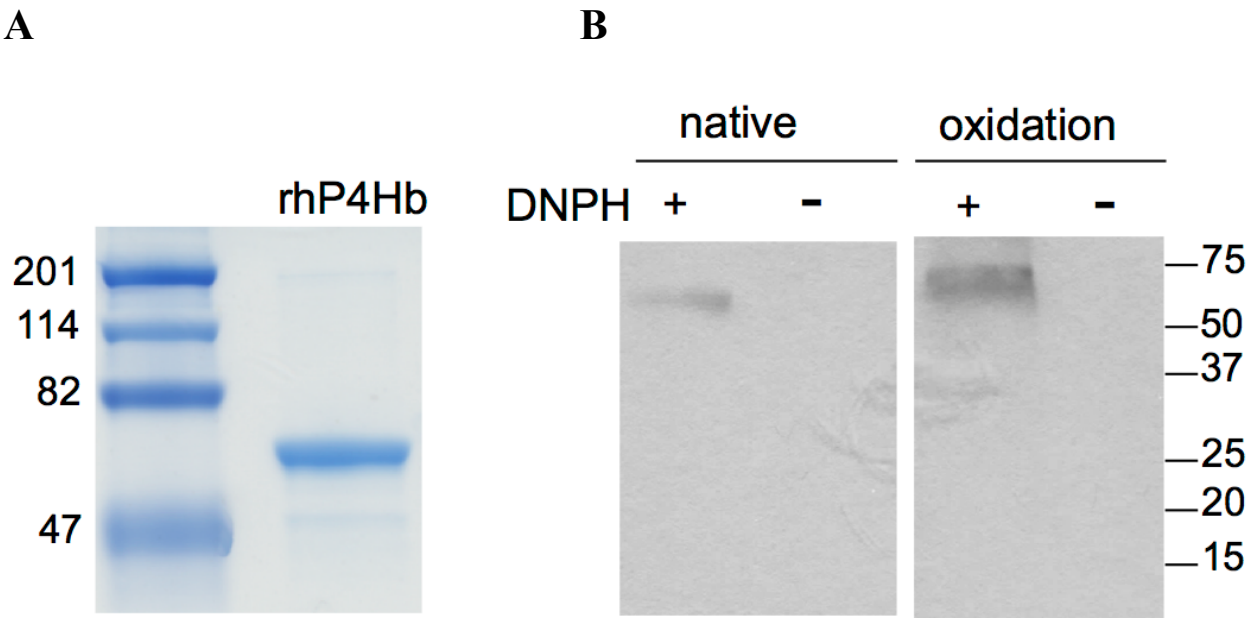

Supplementary Figure 3: The characterization of purified recombinant human P4Hb from hPDI-pTrcHisA clone. (A) Briefly, the hPDI-pTrcHisA plasmid was transformed into BL21(DE3) cells for expression with 0.5 mM IPTG induction. P4Hb was purified from cell lystates using Pro Bond Ni-NTA resin and imidazole elution. Proteins were concentrated with Centriprep YM-30 and judged to be ~95% pure by SDS-PAGE stained with Coomassie Brilliant Blue. Polypeptide molecular weight marker proteins in kDa are shown in the left lane. (B) The purified rhP4Hb was incubated in PBS (native) or PBS containing 100 μM $FeSO_4$, 25mM H_2O_2 and 25mM ascorbate (oxidation) at 37°C for 4 h in the presence or absence of dinitropheylhydrazine. Then the carbonyl modification was analyzed by OxyBlot. The positions of polypeptide molecular weight markers in kDa are on the right edge of the gel.